PROCEEDINGS OF SCIENCE

TeV Halo Study of Geminga and Monogem with HAWC

Ramiro Torres-Escobedo,[a,*] **Hao Zhou,**[a] **Eduardo de la Fuente,**[b] **for the HAWC Collaboration and Mattia di Mauro**[c]

[a] *Tsung-Dao Lee Institute & School of Physics and Astronomy, Shanghai Jiao Tong University*
Shanghai, People's Republic of China
[b] *Departamento de Física, Centro Universitario de Ciencias Exactas e Ingenierias, Universidad de Guadalajara*
Guadalajara, Mexico
[c] *Istituto Nazionale di Fisica Nucleare (INFN)*
Torino, Italy
E-mail: torresramiro350@sjtu.edu.cn, hao_zhou@sjtu.edu.cn, eduardo.delafuente@academicos.udg.mx, dimauro.mattia@gmail.com

Pulsar Inverse Compton halos (TeV halos) are a new subclass of gamma-ray sources. HAWC detected the first two candidates, Geminga and Monogem. These two candidates are of great interest to the anomalous positron excess observed by PAMELA, Fermi-LAT, and AMS-02. This positron excess has been considered to originate from dark matter annihilation, but pulsars can also explain this excess. The HAWC collaboration presented their analysis of the morphology of these pulsars and derived high electron/positron emission efficiency but a diffusion coefficient lower than the average value by a factor of 2 orders of magnitude. Here we present a more in-depth study of Geminga and Monogem with 2139 days of observations from the HAWC observatory. We apply a 3D template model from diffuse-gamma ray electrons/positron emission inverse Compton interactions as they escape the pulsar.

38th International Cosmic Ray Conference (ICRC2023)
26 July - 3 August, 2023
Nagoya, Japan

*Speaker

PoS(ICRC2023)710

1. Introduction

TeV (TeV = 10^{12} eV) halos are a new subclass of gamma-ray (γ-ray) sources, which surround pulsars. The first candidates were first reported by the High Altitude Water Cherenkov (HAWC) collaboration [1]. Two mid-aged pulsars, Geminga and PSR B0656+14 (Monogem) showed an extended diffuse emission of $(5.5 \pm 0.7)^\circ$ and $(4.8 \pm 0.6)^\circ$, respectively. Furthermore, the HAWC collaboration derived a diffusion coefficient of $(4.5 \pm 1.2) \times 10^{27}$ cm^2/s which differs by two orders of magnitude of the average Galactic value.

This launched the search for other halo candidates. The halo candidates have characteristics described in [2]. The evolution of pulsar wind nebulae (PWNe) can be divided into three main stages. The first stage occurs for $t_{age} \lesssim 10$ kiloyears (kyrs) after the supernova explosion (SN). Its remnant drives a strong shock into the surrounding interstellar medium (ISM), which forms a reverse shock (RS). The RS moves radially inwards shocking the inner stellar ejecta. The pulsar drives a pulsar wind that is delimited at the wind termination shock (WTS) forming a pulsar wind nebula. The second evolutionary stage occurs between the ages of $10 \lesssim t_{age} \lesssim 100$ kyrs when the RS reaches the PWN and crushes it. Because the geometry of the SN explosion is often asymmetric, the pulsar receives a kick velocity and displaces significantly from its birth location. The $e^{\pm}$ emission begins to escape into the shocked ejecta and the ISM. The third stages occurs for ages $t_{age} \gtrsim 100$ kyrs when the SNR shock has become subsonic and begins to merge with the ISM. The pulsar has escaped at this point forming a bow-shaped PWNe where $e^{\pm}$ can now escape into the ISM. Geminga and Monogem are the first halo candidates in the third evolutionary stage since they have ages of 343 kyrs and 111 kyrs [3].

The presence of an anomalous positron excess in cosmic ray flux was measured by PAMELA [4], then confirmed by Fermi-LAT and AMS-02 [5, 6]. The positron (e^+) excess in the cosmic ray fraction begins above an energy of 10 GeV (GeV = 10^9 eV). This excess is in disagreement with the population of secondary e^+ generated by cosmic-ray interactions with the (ISM). AMS-02 has furthered measured this excess with high precision up to energies of 1 TeV [7]. Given the high energy losses of $e^{\pm}$, their emission should be located within a few kiloparsec (kpc) [8]. The physical mechanism responsible for this excess remains unanswered. However, dark matter particle mechanisms such as annihilation and decay have been postulated as possible explanations [9]. However, pulsars also present likely contributors to this positron excess [10–12]. Geminga and Monogem are pivotal candidates to explain the above excess, given their proximity to Earth with distances of 0.250 kpc and 0.288 kpc [13], respectively.

We analyze the morphology of two TeV halo candidates, Geminga and Monogem region with 2139 days of the HAWC γ-ray observatory. We study the diffuse emission of these halo candidates with a 3D template model of diffuse γ-ray emission from $e^{\pm}$ as they escape from the pulsar. We show preliminary results of the morphology study and find agreement with the ICS diffuse emission morphology.

2. HAWC Observatory

The High Altitude Water Cherenkov (HAWC γ-ray) observatory is in Puebla, Mexico at an elevation of 4,100 meters above sea level. The HAWC observatory has a primary detector with

300 water Cherenkov detectors (WCDs), each of which houses four photomultiplier tubes (PMTs; one 10" with 3 surrounding 8" PMTs) which yields a detection area of 22,000 m^2/s. This large detection area provides HAWC with an instantaneous field of view (FOV) of 2 sr. Combining this large FOV and the >94% duty cycle allows HAWC to observe 2/3 of the sky everyday. HAWC observes sources with declinations of -26° to $+64^\circ$ in the energy range of 300 GeV - 100 TeV. The operations of the HAWC primary detector are discussed in [14], [15].

The current work uses 2139 days of HAWC data with the "Neural Network" (NN) energy estimator defined in [16], which is optimized for energies >1 TeV. The NN energy estimator utilizes an artificial NN to estimate the energy of γ-rays using shower parameters estimated during HAWC data reconstruction. The data is binned in both fraction of detector present and in bins with quarter decade width in energy. The data presented here is for reconstructed energies of 1 TeV to 316 TeV.

3. Model

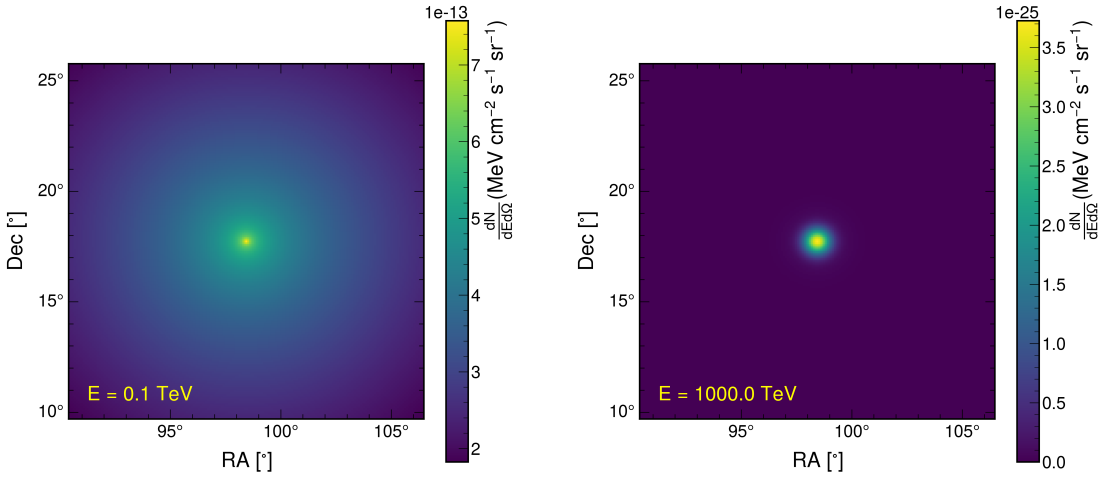

Figure 1: Diffuse γ-ray emission for a diffusion coefficient of $D_0 = 1 \times 10^{26}$ cm^2/s at $e^\pm$ energy of 1 GeV with an injection spectral index of $\alpha = 1.2$. **Left:** Geminga morphology at an energy of 0.1 TeV. **Right:** Geminga morphology at 1000 TeV.

The model is physically motivated as the derived diffuse γ-ray emission from $e^\pm$ comes from inverse Compton scattering (ICS) interactions with cosmic microwave background (CMB), stellar light and infrared light (ISRF) as they escape the pulsar. The $e^\pm$ are injected with a spectral shape of power law with an exponential cutoff at 1000 TeV. The details of γ-ray emission from $e^\pm$ ICS are discussed in [17].

Figure 1 shows templates of diffuse γ-ray emission from electrons/positrons ($e^\pm$) as they escape the pulsar into the interstellar medium (ISM) for a region of $15^\circ \times 15^\circ$ around the pulsar. The left panel shows the more extended morphology an energy of 0.1 TeV that is attributed of $e^\pm$ cooling time that is on the scale of $\gtrsim 10^6$ years (see Figure 3 of [18]). The cooling time scales down to $\gtrsim 10^3$ years for an energy of 1000 TeV. The template contains the γ-ray emission at different

energy bins in the range of 100 GeV to 1000 TeV. Each pixel represents the normalization in units of $\mathrm{MeVcm^{-2}s^{-1}sr^{-1}}$. The normalization is defined as the efficiency in converting the pulsar spin down energy, $\mathrm{K}(\dot{E} \rightarrow e^{\pm})$, to $\mathrm{e}^{\pm}$. The γ-ray emission is generated by a power law with an exponential cutoff at 1000 TeV. The details of the generation of γ-ray emission from $\mathrm{e}^{\pm}$ are discussed in [17].

4. Analysis Approach

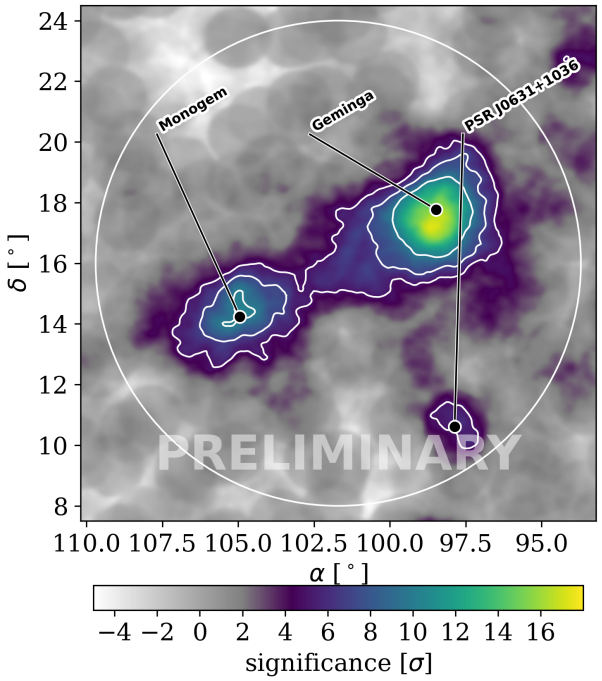

Figure 2: Significance map of the Geminga region for a 1 degree extended disk.

The γ-ray emission can be affected by several parameters including the spectral index, diffusion coefficient, and solid angle over which the integration is performed. We first investigate the effects of three different solid angles for the extended γ-ray emission. Figure 3 shows the γ-ray spectrum for Geminga for different sized regions (left panel) of 10°, 20°, and 30°. The difference in emission for different region sizes is due to the cooling time of $\mathrm{e}^{\pm}$ which is on the order of $\gtrsim 10^6$ years (see Figure 3 of [18]). We utilize the values for γ-ray emission corresponding to solid angle of 30° as to maximize the amount of contained emission for energies between 100 GeV to 1 TeV. The spectrum shown on the right is shown for a solid angle of 30° (right panel) for two diffusion coefficients of $D_0 = 1\times10^{25}$ $\mathrm{cm^2/s}$ and $D_0 = 7.94\times10^{26}$ $\mathrm{cm^2/s}$ both at an $\mathrm{e}^{\pm}$ energy of 1 GeV. There is a difference in the γ-ray emission for energies below 1 TeV which can again attributed to the $\mathrm{e}^{\pm}$ cooling time. For energies above 1 TeV, the differences become negligible with the increasing energy losses. This energy is well within the energy range of the HAWC γ-ray observatory.

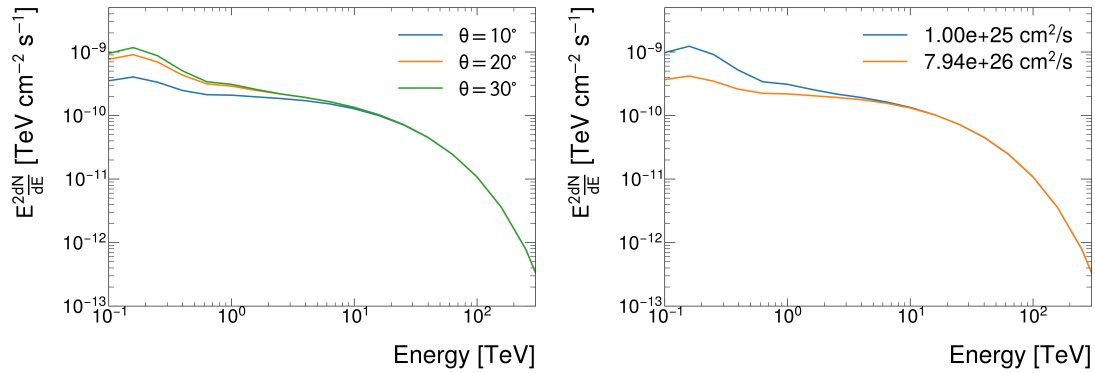

Figure 3: Diffuse γ-ray emission from $e^{\pm}$ ICS. **Left:** Gamma-ray spectrum with a spectral index of α_e=1.5 and a diffusion coefficient $D_0 = 1 \times 10^{26}$ cm^2/s at an $e^{\pm}$ energy of 1 GeV. The γ-ray emission for different regions around the pulsar shown in Figure 1. **Right:** The γ-ray spectrum is shown for different diffusion coefficients.

We normalize the template maps flux values shown in Figure 1 by the flux values integrated over the solid angle of 30° for the corresponding D_0 and α_e. This leaves the pixels in units of 1/sr and allow the spectral shape parameters free to vary during the fit.

In this work, we analyze the diffuse morphology of the TeV halos with templates for diffusion coefficients of 10^{25}-10^{27} cm^2/s at an $e^{\pm}$ energy of 1 GeV. The spectral morphology follows from γ-ray emission from $e^{\pm}$ ICS, which follow a power law with an exponential cutoff with an spectral indexes of $\alpha_e = 0$ to 2.2 with the same shape as presented in Figure 3.

The analysis consists of first interpolating over a grid of templates for parameters, D_0 and α_e. There is a second interpolation over RA$^\circ$ and Dec$^\circ$ per energy bin between 100 GeV to 1000 TeV. Finally, the parameters K($\dot{E} \rightarrow e^{\pm}$), D_0, α_e are fit over the interpolated flux values.

The region of interest is shown in Figure 2. The significance map assumes an extension of 1° degree. In addition to Geminga and Monogem, we see emission from 3HWC J0631-1037 [19], which is associated with PSR J0631+1036. PSR J0631+1036 is a pulsar with an age of 43 kyrs at a distance of 2.1 kpc [3]. Because this source has a significance $\gtrsim 5\sigma$ and it is more distant than Geminga and Monogem, we assume a simple Gaussian spatial morphology model

$$\frac{dN}{d\Omega} = \left(\frac{180}{\pi}\right)^2 \frac{1}{2\pi\sigma^2} \exp\left(-\frac{\theta^2}{\sigma^2}\right), \tag{1}$$

where θ is the angular distance and σ is the Gaussian width. The spectral is a simple power law

$$\phi(E) = \phi_0 \left(\frac{E}{E_0}\right)^{-\alpha}. \tag{2}$$

where ϕ_0 is the normalization in units of TeV^{-1}cm^{-2}s^{-1}, E_0 is the pivot energy, and α is the spectral index. The pivot energy is fixed at 20 TeV.

We fit the morphology of the three sources with the Multi-mission Maximum Likelihood analysis framework (3ML[1]) [20] with the specific HAWC Accelerated Likelihood (HAL) plugin[2].

[1] https://github.com/threeML/threeML
[2] https://github.com/threeML/hawc_hal

The model is implemented via the Astromodels[3] framework, which interacts with 3ML. For each source, we perform a likelihood ratio analysis (test statistic; TS) test defined by the following

$$TS = 2 \ln \frac{\mathcal{L}_{\mathcal{S}+\mathcal{B}}}{\mathcal{L}_{\mathcal{B}}}, \tag{3}$$

where $\mathcal{L}_{\mathcal{S}+\mathcal{B}}$ is the best-fit likelihood of a γ-ray source and background and $\mathcal{L}_{\mathcal{B}}$ is the likelihood of the background only. The validity of the TS statistic with HAWC data is explained in [21].

5. Results

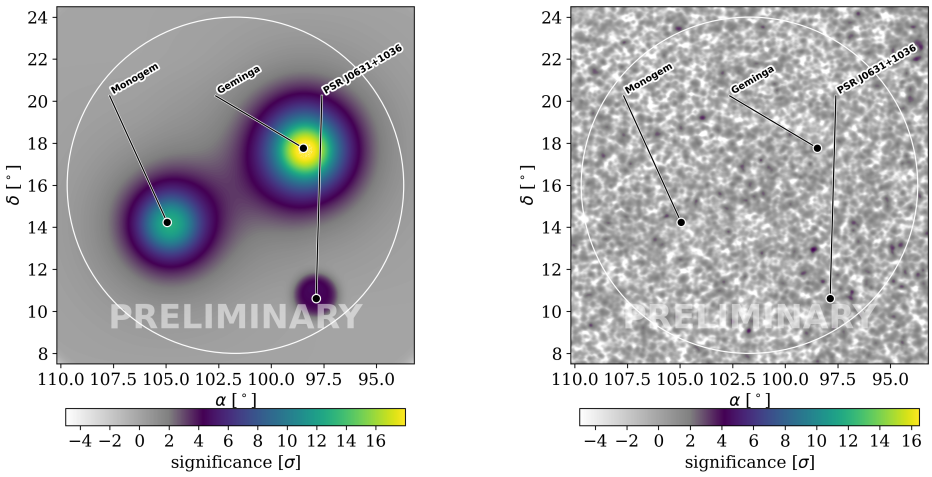

Figure 4: Left: Significance map of the model morphology assuming best-fit parameters with 1° extended disk. **Right:** Significance model map after source subtraction (residual map).

Figure 4 shows significance model (left subpanel) and the residual map (skymap after subtraction from the model; right subpanel). We find this models agrees with the morphology as we see no excess emission in the residual map. The model map is shown in the left panel, assuming the best-fit parameters from the 3ML fit, assumes the morphology of an extended disk of 1°. The residual map is generated for a point source assumption to avoid any pixel cross correlation.

6. Conclusion

The model suggests good agreement with the morphology of Geminga and Monogem. More detections of TeV halos are essential for quantification of diffusion coefficient within the Galaxy. TeV halos are also of great interest in their likely contribution to the local positron excess. We expect the number of TeV halos to increase with observations from current wide field observatories such as HAWC, LHAASO and in the future from SWGO.

[3] https://github.com/threeML/astromodels

7. Acknowledgments

We acknowledge the support from: the US National Science Foundation (NSF); the US Department of Energy Office of High-Energy Physics; the Laboratory Directed Research and Development (LDRD) program of Los Alamos National Laboratory; Consejo Nacional de Ciencia y Tecnología (CONACyT), México, grants 271051, 232656, 260378, 179588, 254964, 258865, 243290, 132197, A1-S-46288, A1-S-22784, CF-2023- I-645, cátedras 873, 1563, 341, 323, Red HAWC, México; DGAPA-UNAM grants IG101323, IN111716-3, IN111419, IA102019, IN106521, IN110621, IN110521 , IN102223; VIEP-BUAP; PIFI 2012, 2013, PROFOCIE 2014, 2015; the University of Wisconsin Alumni Research Foundation; the Institute of Geophysics, Planetary Physics, and Signatures at Los Alamos National Laboratory; Polish Science Centre grant, DEC- 2017/27/B/ST9/02272; Coordinación de la Investigación Científica de la Universidad Michoacana; Royal Society - Newton Advanced Fellowship 180385; Generalitat Valenciana, grant CIDEGENT/2018/034; The Program Management Unit for Human Resources & Institutional Development, Research and Innovation, NXPO (grant number B16F630069); Coordinación General Académica e Innovación (CGAI-UdeG), PRODEP- SEP UDG-CA-499; Institute of Cosmic Ray Research (ICRR), University of Tokyo. H.F. acknowledges support by NASA under award number 80GSFC21M0002. We also acknowledge the significant contributions over many years of Stefan Westerhoff, Gaurang Yodh and Arnulfo Zepeda Dominguez, all deceased members of the HAWC collaboration. Thanks to Scott Delay, Luciano Díaz and Eduardo Murrieta for technical support. R. Torres-Escobedo would like to thank Shanghai Jiao Tong University and the Chinese Scholarship Council and thank the guidance and support of Dr. Hao Zhou, Dr. Eduardo de la Fuente, and Dr. Nural Akchurin.

References

[1] A.U. Abeysekara, A. Albert, R. Alfaro, C. Alvarez, J.D. Álvarez, R. Arceo et al., *Extended gamma-ray sources around pulsars constrain the origin of the positron flux at Earth*, *Science* **358** (2017) .

[2] G. Giacinti, A.M.W. Mitchell, R. López-Coto, V. Joshi, R.D. Parsons and J.A. Hinton, *Halo fraction in TeV-bright pulsar wind nebulae*, *Astronomy and Astrophysics* **636** (2020) .

[3] R.N. Manchester, G.B. Hobbs, A. Teoh and M. Hobbs, *The australia telescope national facility pulsar catalogue*, astro-ph/0412641.

[4] O. Adriani, G.C. Barbarino, G.A. Bazilevskaya, R. Bellotti, M. Boezio, E.A. Bogomolov et al., *Observation of an anomalous positron abundance in the cosmic radiation*, 0810.4995.

[5] M. Ackermann, M. Ajello, A. Allafort, W.B. Atwood, L. Baldini, G. Barbiellini et al., *Measurement of Separate Cosmic-Ray Electron and Positron Spectra with the Fermi Large Area Telescope*, *Physical Review Letters* **108** (2012) .

[6] O. Adriani, G.C. Barbarino, G.A. Bazilevskaya, R. Bellotti, A. Bianco, M. Boezio et al., *Cosmic-Ray Positron Energy Spectrum Measured by PAMELA*, *Phys. Rev. Lett.* **111** (2013) 081102.

[7] AMS Collaboration collaboration, *Towards understanding the origin of cosmic-ray positrons*, *Phys. Rev. Lett.* **122** (2019) 041102.

[8] M. Di Mauro, F. Donato, N. Fornengo, R. Lineros and A. Vittino, *Interpretation of AMS-02 electrons and positrons data*, *JCAP* **04** (2014) 006 [1402.0321].

[9] A. Ibarra, A.S. Lamperstorfer and J. Silk, *Dark matter annihilations and decays after the AMS-02 positron measurements*, *Phys. Rev. D* **89** (2014) 063539 [1309.2570].

[10] A.M. Atoyan, F.A. Aharonian and H.J. Völk, *Electrons and positrons in the galactic cosmic rays*, *Phys. Rev. D* **52** (1995) 3265.

[11] L. Zhang and K.S. Cheng, *Cosmic-ray positrons from mature gamma-ray pulsars*, *A&A* **368** (2001) 1063.

[12] H. Yüksel, M.D. Kistler and T. Stanev, *TeV Gamma Rays from Geminga and the Origin of the GeV Positron Excess*, *Physical Review Letters* **103** (2009) 051101.

[13] H.E.S.S. Collaboration, H. Abdalla, A. Abramowski, F. Aharonian, F. Ait Benkhali, A.G. Akhperjanian et al., *The population of TeV pulsar wind nebulae in the H.E.S.S. Galactic Plane Survey*, *A&A* **612** (2018) A2.

[14] A.J. Smith, *HAWC: Design, Operation, Reconstruction and Analysis*, in *Proceedings of The 34th International Cosmic Ray Conference — PoS(ICRC2015)*, (Trieste, Italy), p. 966, Sissa Medialab, 2016, DOI.

[15] A.U. Abeysekara, A. Albert, R. Alfaro, C. Alvarez, J.D. Álvarez, M. Araya et al., *The High-Altitude Water Cherenkov (HAWC) observatory in México: The primary detector*, *Nuclear Instruments and Methods in Physics Research Section A: Accelerators, Spectrometers, Detectors and Associated Equipment* **1052** (2023) 168253.

[16] A.U. Abeysekara, A. Albert, R. Alfaro, C. Alvarez, J.D. Álvarez, J.R.A. Camacho et al., *Measurement of the Crab Nebula Spectrum Past 100 TeV with HAWC*, *The Astrophysical Journal* **881** (2019) 134.

[17] M. Di Mauro, S. Manconi and F. Donato, *Detection of a γ-ray halo around Geminga with the Fermi-LAT data and implications for the positron flux*, *Physical Review D* **100** (2019) .

[18] R.-Y. Liu, *The Physics of Pulsar Halos: Research Progress and Prospect*, 2207.04011.

[19] A. Albert, R. Alfaro, C. Alvarez, J.R.A. Camacho, J.C. Arteaga-Velázquez, K.P. Arunbabu et al., *3HWC: The Third HAWC Catalog of Very-high-energy Gamma-Ray Sources*, *The Astrophysical Journal* **905** (2020) 76 [2007.08582].

[20] G. Vianello, R.J. Lauer, P. Younk, L. Tibaldo, J.M. Burgess, H. Ayala et al., *The Multi-Mission Maximum Likelihood framework (3ML)*, 1507.08343.

[21] A.U. Abeysekara, A. Albert, R. Alfaro, C. Alvarez, J.D. Álvarez, R. Arceo et al., *The 2HWC HAWC Observatory Gamma-Ray Catalog*, *The Astrophysical Journal* **843** (2017) .

Full Authors List: HAWC Collaboration

A. Albert[1], R. Alfaro[2], C. Alvarez[3], A. Andrés[4], J.C. Arteaga-Velázquez[5], D. Avila Rojas[2], H.A. Ayala Solares[6], R. Babu[7], E. Belmont-Moreno[2], K.S. Caballero-Mora[3], T. Capistrán[4], S. Yun-Cárcamo[8], A. Carramiñana[9], F. Carreón[4], U. Cotti[5], J. Cotzomi[26], S. Coutiño de León[10], E. De la Fuente[11], D. Depaoli[12], C. de León[5], R. Diaz Hernandez[9], J.C. Díaz-Vélez[11], B.L. Dingus[1], M. Durocher[1], M.A. DuVernois[10], K. Engel[8], C. Espinoza[2], K.L. Fan[8], K. Fang[10], N.I. Fraija[4], J.A. García-González[13], F. Garfias[4], H. Goksu[12], M.M. González[4], J.A. Goodman[8], S. Groetsch[7], J.P. Harding[1], S. Hernandez[2], I. Herzog[14], J. Hinton[12], D. Huang[7], F. Hueyotl-Zahuantitla[3], P. Hüntemeyer[7], A. Iriarte[4], V. Joshi[28], S. Kaufmann[15], D. Kieda[16], A. Lara[17], J. Lee[18], W.H. Lee[4], H. León Vargas[2], J. Linnemann[14], A.L. Longinotti[4], G. Luis-Raya[15], K. Malone[19], J. Martínez-Castro[20], J.A.J. Matthews[21], P. Miranda-Romagnoli[22], J. Montes[4], J.A. Morales-Soto[5], M. Mostafá[6], L. Nellen[23], M.U. Nisa[14], R. Noriega-Papaqui[22], L. Olivera-Nieto[12], N. Omodei[24], Y. Pérez Araujo[4], E.G. Pérez-Pérez[15], A. Pratts[2], C.D. Rho[25], D. Rosa-Gonzalez[9], E. Ruiz-Velasco[12], H. Salazar[26], D. Salazar-Gallegos[14], A. Sandoval[2], M. Schneider[8], G. Schwefer[12], J. Serna-Franco[2], A.J. Smith[8], Y. Son[18], R.W. Springer[16], O. Tibolla[15], K. Tollefson[14], I. Torres[9], R. Torres-Escobedo[27], R. Turner[7], F. Ureña-Mena[9], E. Varela[26], L. Villaseñor[26], X. Wang[7], I.J. Watson[18], F. Werner[12], K. Whitaker[6], E. Willox[8], H. Wu[10], H. Zhou[27]

[1]Physics Division, Los Alamos National Laboratory, Los Alamos, NM, USA, [2]Instituto de Física, Universidad Nacional Autónoma de México, Ciudad de México, México, [3]Universidad Autónoma de Chiapas, Tuxtla Gutiérrez, Chiapas, México, [4]Instituto de Astronomía, Universidad Nacional Autónoma de México, Ciudad de México, México, [5]Instituto de Física y Matemáticas, Universidad Michoacana de San Nicolás de Hidalgo, Morelia, Michoacán, México, [6]Department of Physics, Pennsylvania State University, University Park, PA, USA, [7]Department of Physics, Michigan Technological University, Houghton, MI, USA, [8]Department of Physics, University of Maryland, College Park, MD, USA, [9]Instituto Nacional de Astrofísica, Óptica y Electrónica, Tonantzintla, Puebla, México, [10]Department of Physics, University of Wisconsin-Madison, Madison, WI, USA, [11]CUCEI, CUCEA, Universidad de Guadalajara, Guadalajara, Jalisco, México, [12]Max-Planck Institute for Nuclear Physics, Heidelberg, Germany, [13]Tecnologico de Monterrey, Escuela de Ingeniería y Ciencias, Ave. Eugenio Garza Sada 2501, Monterrey, N.L., 64849, México, [14]Department of Physics and Astronomy, Michigan State University, East Lansing, MI, USA, [15]Universidad Politécnica de Pachuca, Pachuca, Hgo, México, [16]Department of Physics and Astronomy, University of Utah, Salt Lake City, UT, USA, [17]Instituto de Geofísica, Universidad Nacional Autónoma de México, Ciudad de México, México, [18]University of Seoul, Seoul, Rep. of Korea, [19]Space Science and Applications Group, Los Alamos National Laboratory, Los Alamos, NM USA [20]Centro de Investigación en Computación, Instituto Politécnico Nacional, Ciudad de México, México, [21]Department of Physics and Astronomy, University of New Mexico, Albuquerque, NM, USA, [22]Universidad Autónoma del Estado de Hidalgo, Pachuca, Hgo., México, [23]Instituto de Ciencias Nucleares, Universidad Nacional Autónoma de México, Ciudad de México, México, [24]Stanford University, Stanford, CA, USA, [25]Department of Physics, Sungkyunkwan University, Suwon, South Korea, [26]Facultad de Ciencias Físico Matemáticas, Benemérita Universidad Autónoma de Puebla, Puebla, México, [27]Tsung-Dao Lee Institute and School of Physics and Astronomy, Shanghai Jiao Tong University, Shanghai, China, [28]Erlangen Centre for Astroparticle Physics, Friedrich Alexander Universität, Erlangen, BY, Germany

PoS(ICRC2023)710